JOC The Journal of Organic Chemistry

Article

pubs.acs.org/joc

Activation-Strain Analysis Reveals Unexpected Origin of Fast Reactivity in Heteroaromatic Azadiene Inverse-Electron-Demand Diels–Alder Cycloadditions

Austin Talbot,[†] Deepa Devarajan,[†] Samantha J. Gustafson,[†] Israel Fernández,[‡] F. Matthias Bickelhaupt,*[,§,∥] and Daniel H. Ess*[,†]

[†]Department of Chemistry and Biochemistry, Brigham Young University, Provo, Utah 84602, United States

[‡]Departamento de Química Orgánica I, Facultad de Ciencias Químicas, Universidad Complutense, E-28040 Madrid, Spain

[§]Department of Theoretical Chemistry and Amsterdam Center for Multiscale Modeling (ACMM), VU University Amsterdam, De Boelelaan 1083, NL-1081 HV Amsterdam, The Netherlands

[∥]Institute for Molecules and Materials (IMM), Radboud University Nijmegen, Heyendaalseweg 135, NL-6525 AJ Nijmegen, The Netherlands

Supporting Information

ABSTRACT: Heteroaromatic azadienes, especially 1,2,4,5-tetrazines, are extremely reactive partners with alkenes in inverse-electron-demand Diels–Alder reactions. Azadiene cycloaddition reactions are used to construct heterocycles in synthesis and are popular as bioorthogonal reactions. The origin of fast azadiene cycloaddition reactivity is classically attributed to the inverse frontier molecular orbital (FMO) interaction between the azadiene LUMO and alkene HOMO. Here, we use a combination of ab initio, density functional theory, and activation-strain model calculations to analyze physical interactions in heteroaromatic azadiene–alkene cycloaddition transition states. We find that FMO interactions do not control reactivity because, while the inverse FMO interaction becomes more stabilizing, there is a decrease in the forward FMO interaction that is offsetting. Rather, fast cycloadditions are due to a decrease in closed-shell Pauli repulsion between cycloaddition partners. The kinetic–thermodynamic relationship found for these inverse-electron-demand cycloadditions is also due to the trend in closed-shell repulsion in the cycloadducts. Cycloaddition regioselectivity, however, is the result of differences in occupied–unoccupied orbital interactions due to orbital overlap. These results provide a new predictive model and correct physical basis for heteroaromatic azadiene reactivity and regioselectivity with alkene dieneophiles.

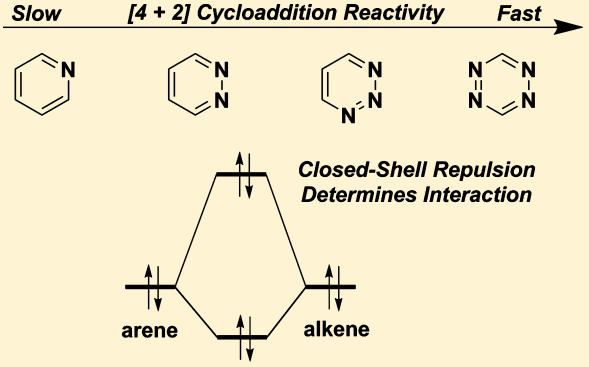

INTRODUCTION

The use of heteroaromatic azadienes (Scheme 1a) in inverse-electron-demand Diels–Alder reactions provides an efficient methodology for construction of heterocycles.[1−3] This type of reaction usually involves [4 + 2] cycloaddition with alkenes, followed by retrocycloaddition (Scheme 1b). Boger and co-workers have developed useful synthetic routes to a variety of azadienes and examined their reaction scope, substituent effects, and regioselectivity with alkene cycloaddition partners.[1,4,5] Boger and co-workers have also used heteroaromatic azadiene cycloadditions in the total synthesis of streptonigrin,[6] phosphodiesterase inhibitors,[7] trikentrin A,[8] several marine natural products,[9] and *Amaryllidaceae* alkaloids.[10] Several screening libraries also utilize azadiene Diels–Alder reactions.[11]

Heteroaromatic azadiene Diels–Alder reactions have become popular as bioorthogonal reactions due to their very fast "click-like" reactivity (Scheme 1c).[12−16] The most widely used azadiene for bioorthogonal reactions is 1,2,4,5-tetrazine.[17] For example, Fox and co-workers showed that 3,6-di-(2-pyridyl)-*s*-tetrazine reacts with *trans*-cyclooctene functionalized with thioredoxin in less than 5 min and with complete conversion (Scheme 1c).[13,18]

The very fast reactivity of 1,2,4,5-tetrazines and other heteroaromatic azadienes in [4 + 2] cycloadditions with alkenes is classically attributed to an enhanced frontier molecular orbital (FMO)[19] interaction (Scheme 2).[1,20] In this FMO model, the electron-deficient azadiene has a highly stabilized lowest unoccupied molecular orbital (LUMO) and the inverse FMO energy gap with the alkene highest occupied molecular orbital (HOMO) is small, which, upon interaction, leads to significant electron delocalization from the alkene to the azadiene with concomitant energy stabilization. This single FMO interaction is assumed to more than compensate for the

Received: November 7, 2014
Published: December 4, 2014

 © 2014 American Chemical Society dx.doi.org/10.1021/jo5025514 | *J. Org. Chem.* 2015, 80, 548–558

Scheme 1. (a) Representative examples of Heteroaromatic Azadienes (b) Example of a Diels–Alder Cycloaddition and Retrocycloaddition Reaction between 3,6-Disubstituted 1,2,4,5-Tetrazine and Ethylene (c) Example of a Heteroaromatic Azadiene Bioorthogonal Reaction

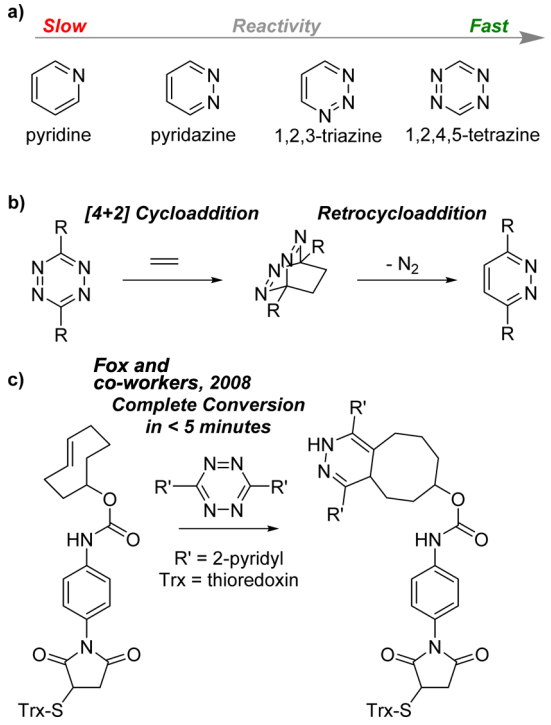

Scheme 2. Comparison of FMO Energy Gaps for (a) a Nonpolarized Diels–Alder Reaction versus (b) a Fast Azadiene Inverse-Demand Diels–Alder Reaction

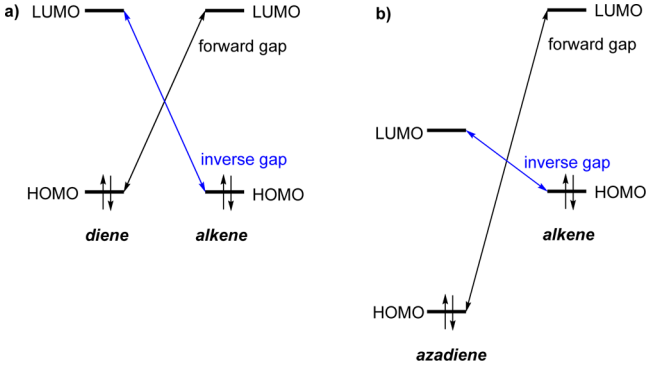

increase in the forward FMO energy gap between the azadiene HOMO and the alkene LUMO (Scheme 2).[21−23]

This FMO interpretation continues to be prominently used to explain the reactivity of cycloadditions with heteroaromatic azadienes.[24,25] For example, the lower activation energy of tetrazine versus azide with *trans*-cyclooctene, cyclooctyne, and dibenzocyclooctyne is attributed to this FMO interaction.[26] Similarly, tetrazine reactivity with alkynylboronates is rationalized by FMO energies.[27,28] While this FMO explanation for azadiene reactivity is appealing, it has only been supported by calculation of ground-state π orbital energies.[29] Evaluation of transition-state energy stabilization resulting from occupied-to-unoccupied orbital interactions (i.e., electron delocalization) has not been computationally tested. It is well-known that the FMO model outlined in Scheme 2, applied within the context of perturbation theory,[30] also neglects reaction coordinate geometry changes, molecular orbital distortions, closed-shell repulsion (also called Pauli or exchange repulsion), and electrostatic interactions.[31] Here, we use a combination of ab initio, density functional theory, and activation-strain calculations to analyze orbital energy stabilization that is akin to perturbation-style FMO interactions. Surprisingly, we find that occupied–unoccupied orbital interactions are not the origin of fast heteroaromatic azadiene Diels–Alder cycloadditions. Rather, the fast reactivity is due to a decrease in closed-shell electron–electron repulsion between the azadiene and the alkene. Closed-shell repulsion is also the origin of the kinetic–thermodynamic relationship in azadiene–alkene cycloadditions. However, regioselectivity is due to a difference in occupied–unoccupied orbital interactions. These results provide a new model and correct physical basis for understanding and designing heteroaromatic azadiene reactivity and regioselectivity for cycloadditions with alkenes.

RESULTS/DISCUSSION

Method to Examine Orbital Interactions in Inverse-Electron-Demand Diels–Alder Cycloaddition Reactions. FMO theory applied within the context of perturbation theory only considers a portion of the total physical interactions between reacting cycloaddition partners. The intermolecular interaction of two cycloaddition partners involves: (1) Coulombic/electrostatic attraction and repulsion between electrons and nuclei, (2) closed-shell repulsion between filled orbitals, which is termed exchange repulsion or Pauli repulsion, and (3) occupied–unoccupied orbital (electron delocalization) interactions. Typically, FMO theory neglects electrostatic interactions and closed-shell repulsion[30,31] and only the frontier ground-state filled-empty orbital interactions are assumed to determine reactivity as cycloaddition partners begin to react.

Activation-strain analysis[32−34] offers the ability to analyze cycloaddition transition states or any other structure along the reaction coordinate,[35] rather than only ground states, in a chemically intuitive context that closely parallels the perturbation approach of FMO theory. Activation-strain analysis also allows direct analysis of intermolecular interactions and the resulting energy stabilization, including occupied–unoccupied orbital interactions. Equation 1 defines the total cycloaddition transition-state activation energy and its decomposition into a strain-energy term associated with the geometrical deformation that the reactants undergo ($\Delta E^{\ddagger}_{\mathrm{STRAIN}}$) along with a term for the interaction between these deformed reactants ($\Delta E^{\ddagger}_{\mathrm{INT}}$). Analysis of transition-state structures in this fashion is part of the activation-strain model developed and popularized by the Houk[36] and Bickelhaupt[37] groups. For heteroaromatic azadiene cycloadditions, $\Delta E^{\ddagger}_{\mathrm{STRAIN}}$ is the strain-energy penalty to alter the heteroaromatic azadiene and alkene from their ground-state structures into their transition-state geometries. $\Delta E^{\ddagger}_{\mathrm{INT}}$ is the interaction energy between the distorted cycloaddition fragments and controls the extent of geometric change required by the reactants. The strain and interaction energy terms are graphically depicted in Scheme 3 for the reaction of 1,2,4,5-tetrazine with ethylene.

$$\Delta E^{\ddagger} = \Delta E^{\ddagger}_{\mathrm{STRAIN}} + \Delta E^{\ddagger}_{\mathrm{INT}} \quad (1)$$

The connection to FMO theory is found in eq 2 with the dissection of the intermolecular interaction energy between distorted cycloaddition fragments into contributions from

dx.doi.org/10.1021/jo5025514 | J. Org. Chem. 2015, 80, 548−558

Scheme 3. Graphical Depiction of Activation-Strain Energy ($\Delta E^{\ddagger}_{STRAIN}$) and Interaction Energy ($\Delta E^{\ddagger}_{INT}$) for the Cycloaddition of 1,2,4,5-Tetrazine with Ethylene

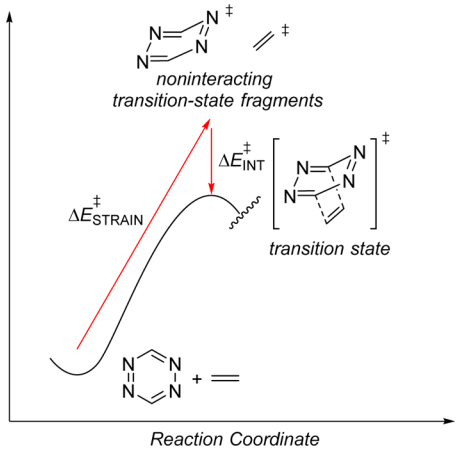

electrostatic interactions ($\Delta E^{\ddagger}_{ELSTAT}$), closed-shell or Pauli repulsion ($\Delta E^{\ddagger}_{PAULI}$), and occupied−unoccupied orbital interactions ($\Delta E^{\ddagger}_{ORB}$).[34] Quasiclassical electrostatic interactions include nuclei−nuclei, nuclei−electron, and electron−electron interactions between transition-state fragments. Closed-shell repulsion between filled cycloaddition fragments arise from the requirement of same-spin electrons to obey the Pauli exclusion principle. This is often visualized by a 4-electron, 2-orbital interaction diagram shown in Chart 1a where the total interaction is net repulsive. The orbital interaction term is composed of intermolecular occupied-to-vacant orbital interactions and minor intramolecular polarization. These orbital interactions describe electron delocalization (also termed charge transfer) from one cycloaddition partner to the other. This is also visualized by the classic 2-electron, 2-orbital interaction diagram between a doubly occupied orbital and an unoccupied orbital (Chart 1b).

$$\Delta E^{\ddagger}_{INT} = \Delta E^{\ddagger}_{ELSTAT} + \Delta E^{\ddagger}_{PAULI} + \Delta E^{\ddagger}_{ORB} \quad (2)$$

COMPUTATIONAL DETAILS

All ground-state and transition-state geometries were optimized with Gaussian 09[38] using the BP86 density functional combined with the 6-31G(d,p) basis set. CCSD(T) calculations, which provide a high-accuracy comparison, were also carried out in Gaussian 09. Activation-strain analysis was carried out using the Amsterdam Density Functional (ADF)[39] program with the BP86 functional in conjunction with the TZP basis set, which is a Slater-type orbital triple-ξ quality basis set with one set of polarization functions on each atom: 2p on H; 3d on C and N. The activation-strain analysis trends are independent of the functional and basis set. Analysis of orbital energies with deletion of all unoccupied orbitals was also carried out in ADF.

Transition-State Geometries and Activation Energy Trend. To identify the origin of fast cycloaddition reactivity for 1,2,4,5-tetrazine and similar heteroaromatic azadienes with alkenes, we examined reactions 1−5 shown in Scheme 4. This set of reactions evaluates the impact of successively replacing an arene methine CH group with a more electronegative nitrogen atom. This set of reactions is also useful to examine regioselective addition of ethylene, such as 3,6-addition versus 1,4-addition for 1,2,4,5-tetrazine.

Scheme 4. Reactions Investigated

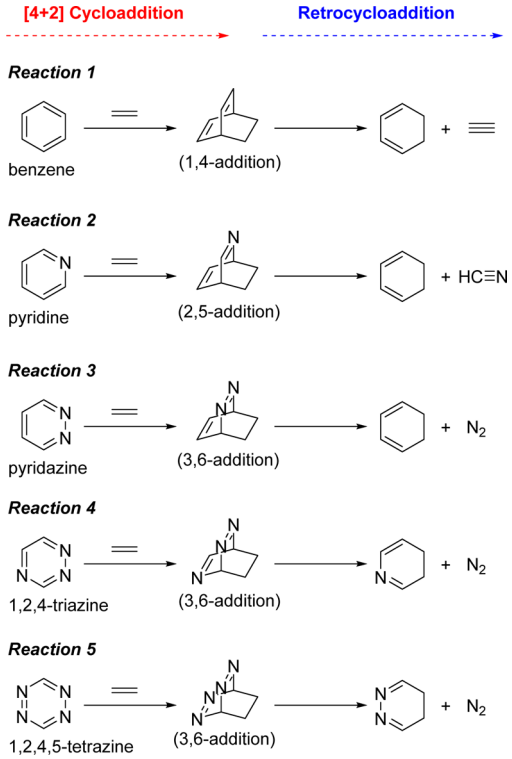

In 2005, Ho and Li reported G3(MP2) transition states for reactions 1−5.[40−42] This work showed that nitrogen atom substitution decreases the activation barrier for cycloaddition,

Chart 1. Graphical Depiction of (a) Closed-Shell Pauli Repulsion and (b) Occupied−Unoccupied Orbital Stabilization

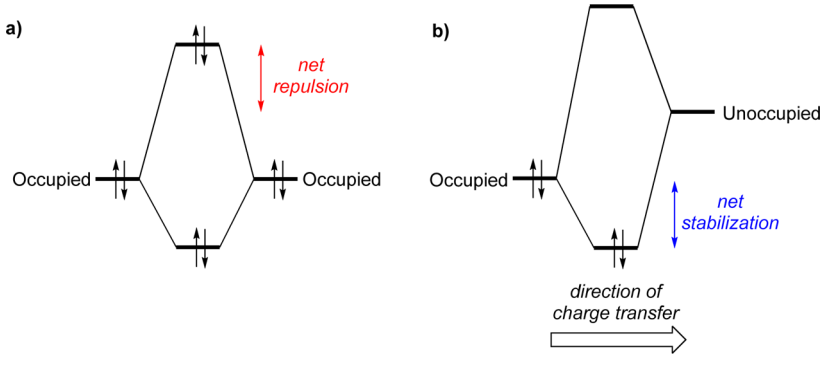

dx.doi.org/10.1021/jo5025514 | J. Org. Chem. 2015, 80, 548−558

but no rationale for reactivity was discussed. Regioselective preference for C−C bond formation over C−N bond formation was attributed to more efficient orbital overlap and a more stabilizing resonance integral.[43] More recently, in 2009, Hayden and Houk reported B3LYP transition states for a series of heteroaromatic azadienes with ethylene.[44] This report showed a linear correlation between activation enthalpies with reaction enthalpies (Bell−Evans−Polanyi correlation)[45] and with activation strain (or distortion) energies.

Figure 1 portrays the lowest energy regioisomeric BP86 transition-state structures, which are similar to transition-state

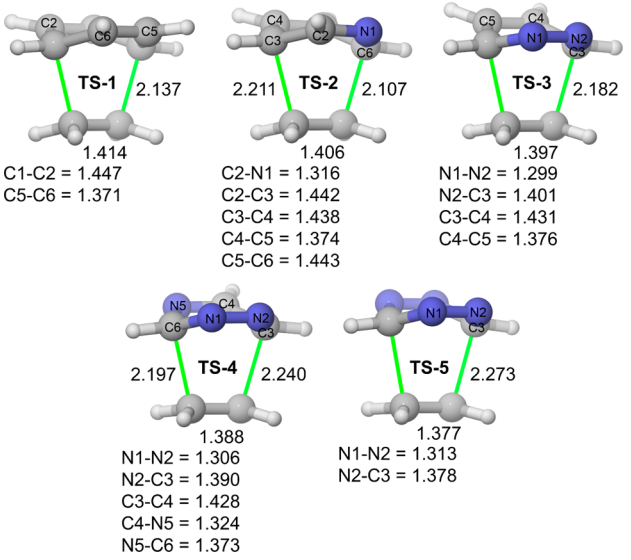

Figure 1. BP86/6-31G(d,p) transition-state geometries. Bond lengths reported in Å.

geometries previously reported.[40,44] These transition states are displayed to showcase the change from shorter to longer partial forming C−C bond lengths, i.e., late-to-early geometry progression, as nitrogen atoms are introduced into the arene ring system. For example, in **TS-1**, the partial forming C−C bond lengths are 2.137 Å and increase to 2.273 Å in **TS-5**. This earlier transition-state geometry for 1,2,4,5-tetrazine compared to benzene is also portrayed in the ethylene C−C bond lengths. In **TS-1**, the ethylene bond length is 1.414 Å and is 1.377 Å in **TS-5**.

The calculated activation energies ($\Delta E^{\ddagger}$) corresponding to the structures in Figure 1 are reported in Table 1 and graphically displayed in Figure 2. In accordance with previous

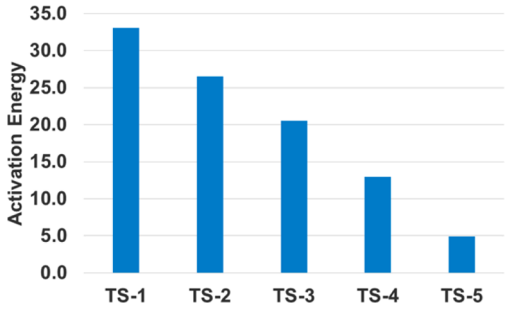

Figure 2. Trend in $\Delta E^{\ddagger}$ values (kcal/mol).

work by Ho et al.[40] and Hayden and Houk,[44] the $\Delta E^{\ddagger}$ values show a significant and nearly monotonic decrease in activation barrier of ∼6−7 kcal/mol with the successive introduction of nitrogen atoms.

To verify the calculated trend in activation energies, we also examined CCSD(T)/6-311+G(2d,p) energies. Indeed, there is a strong linear correlation between BP86/6-31G(d,p) and CCSD(T)/6-311+G(2d,p)//BP86/6-31G(d,p) activation energies with an R^2 of 0.99 (see the Supporting Information).

Table 1 also reports the $\Delta E^{\ddagger}$ values for higher energy regioisomeric transition states. There is a very large energy preference, ranging from ∼10−15 kcal/mol, for forming two C−C bonds versus forming C−C/C−N or C−N/C−N bonds.

Reaction Energy Landscapes. We also explored the energies of the cycloadduct and subsequent retrocycloaddition to release either HCCH, HCN, or N_2. The complete reaction energy landscapes are shown in Figure 3. Similar to previous work, this plot shows the connection between activation energies and reaction energies.[44] The $\Delta E^{\ddagger}$ vs ΔE_{rxn} linear correlation is given as $\Delta E^{\ddagger} = 0.76*\Delta E_{rxn} + 28.2$ kcal/mol with an R^2 value of 0.99 (see the Supporting Information). The second apparent feature of these energy landscapes is that, for benzene and pyridine, the retrocycloaddition activation energy is larger than the initial cycloaddition activation barrier. For reactions 3−5, the cycloadduct is exothermic and the barrier for retrocycloaddition is lower than initial cycloaddition. Previously, Birney and co-workers found that tetrazine cycloadditions with alkynes is rate-limiting and subsequent deazetization via retrocycloaddition is very rapid and potentially barrierless.[46]

One possible explanation for the kinetic−thermodynamic relationship is that the π aromaticity in heteroaromatic azadienes is altered upon cycloaddition. We have discounted this possibility because Schleyer showed that calculated

Table 1. BP86 Activation Barriers[a,d]

transition-state structure	$\Delta E^{\ddagger}_{(BP86)}$	$\Delta E^{\ddagger}_{(CCSD(T))}$[c]	$\Delta E_{RXN(BP86)}$	$\Delta E_{RXN(CCSD(T))}$[c]
TS-1	33.1 (34.6)[b]	32.6	6.5	0.3
TS-2 (pyridine: 2,5-addition)	26.5 (28.2)[b]	26.9	−1.5	−6.9
(pyridine:1,4-addition)	41.5 (42.9)[b]			
TS-3 (pyridazine: 3,6-addition)	20.5 (22.3)[b]	22.1	−11.3	−14.5
(pyridazine:1,4-addition)	30.3 (32.0)[b]			
TS-4 (1,2,4-triazine: 3,6-addition)	12.9 (15.0)[b]	15.8	−19.6	−21.3
(1,2,4-triazine: 1,4-addition)	37.0 (38.6)[b]			
(1,2,4-triazine: 2,5-addition)	21.0 (23.0)[b]			
TS-5 (1,2,4,5-tetrazine: 3,6-addition)	4.9 (7.1)[b]	9.2	−30.2	−28.8
(1,2,4,5-tetrazine: 1,4-addition)	21.6 (23.7)[b]			

[a]6-31G(d,p) basis set. [b]Zero-point energy corrected. [c]6-311+G(2d,p) basis set. [d]Energies are reported in kcal/mol.

dx.doi.org/10.1021/jo5025514 | J. Org. Chem. 2015, 80, 548−558

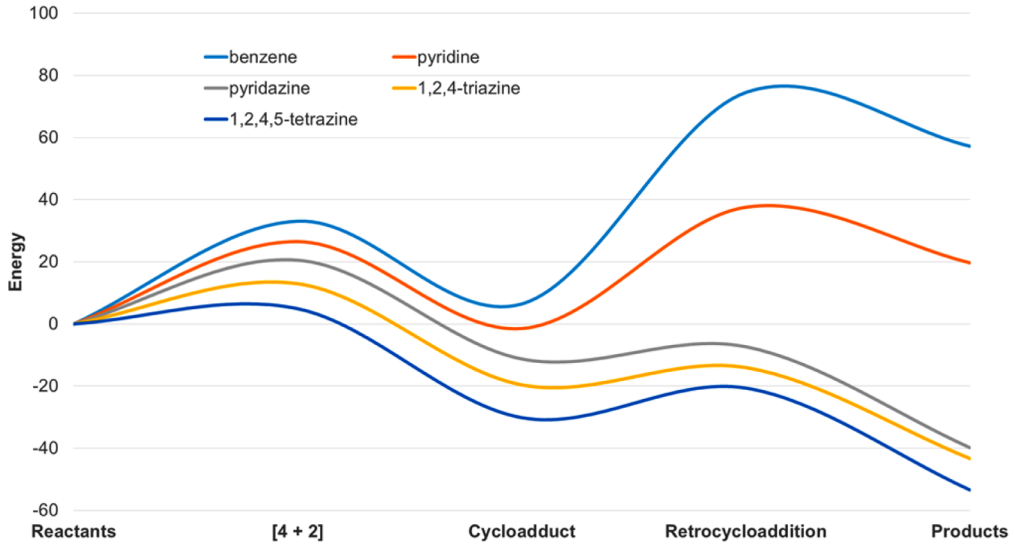

Figure 3. BP86/6-31G(d,p) energy landscapes. Energies reported in kcal/mol.

Table 2. BP86/6-31G(d,p) Energies and BP86/TZP Energy Dissection Analysis on Geometries Constrained to Have Forming Partial C−C Bond Lengths at 2.2 Å[f]

	ΔE^a	$\Delta E_{STRAIN}{}^a$	$\Delta E_{INT}{}^a$	$\Delta E_{ORB}{}^b$	$\Delta E_{ELSTAT}{}^b$	$\Delta E_{PAULI}{}^b$	$\Delta E_{INT}{}^b$	S^e
Rxn 1: benzene (1,4-addition)	32.5	29.7 [20.9[c], 8.8[d]]	2.7	−55.3	−54.2	114.0	4.5	0.20
Rxn 2: pyridine (2,5-addition)	26.4	27.8 [19.9[c], 7.9[d]]	−1.4	−55.3	−52.2	108.0	0.5	0.21
Rxn 3: pyridazine (3,6-addition)	20.5	25.6 [18.9[c], 6.7[d]]	−5.2	−54.9	−49.7	101.6	−3.0	0.22
Rxn 4: 1,2,4-triazine (3,6-addition)	12.9	22.9 [16.7[c], 6.2[d]]	−8.1	−55.5	−47.7	95.6	−7.6	0.22
Rxn 5: 1,2,4,5-tetrazine (3,6-addition)	4.6	18.8 [13.4[c], 5.4[d]]	−14.3	−55.8	−45.3	89.3	−11.8	0.23

[a]BP86/6-31G(d,p). [b]BP86/TZP. [c]Diene activation-strain energy. [d]Ethylene activation-strain energy. [e]Orbital overlap between alkene HOMO and heteroazadiene LUMO. [f]Energies are reported in kcal/mol.

magnetic and energetic quantities for the aromaticity of benzene and heteroaromatic azines are nearly identical.[47−51]

Another possibility for the kinetic−thermodynamic relationship is that lower energy transition states develop more cyclic aromaticity upon bond formation (not π aromaticity).[52,53] To evaluate this possibility, similar to previous studies of aromatic transition states,[54,55] we calculated the nuclear independent chemical shift (NICS)[56] values at the [3,+1] ring critical point of the electron density.[57] All of the transition states have large negative NICS values, and the NICS values are less negative with more nitrogen atoms. For example, **TS-2** and **TS-5** have NICS values of −24.8 and −21.8 ppm, respectively. Anisotropy of the induced current density (ACID) also confirms the relative aromaticity.[58] This result suggests that the magnetic transition-state aromaticity decreases with more nitrogen atoms and is unlikely an explanation for the reactivity and thermodynamic trends.

Activation-Strain Analysis. Because the transition-state geometries shift from late to early, an equitable comparison of reactions based on energy decomposition analysis should be done using a consistent geometry. We chose to analyze transition-state-like geometries with forming partial C−C bond lengths constrained to 2.2 Å. Analysis of transition-state energies is reported in the Supporting Information. Importantly, 2.2 Å geometries give energies very close to the transition-state energies. For example, the $\Delta E^{\ddagger}$ for 1,4-addition of ethylene to benzene is 33.1 kcal/mol. Using the 2.2 Å geometry decreases the energy to 32.5 kcal/mol. Similarly, the 3,6-addition of ethylene to 1,2,4,5-tetrazine at fixed 2.2 Å partial bond lengths is 4.6 kcal/mol, which is only 0.3 kcal/mol less than the 4.9 kcal/mol $\Delta E^{\ddagger}$ value. In general, the 2.2 Å geometries have energies within 1 kcal/mol of the activation energies. More importantly, the trend in 2.2 Å geometry energies mirrors the trend in activation energies. Also, constraining the bond lengths at 2.0 and 2.4 Å, which are the extremes of the possible early and late transition-state positions, results in similar trends.

Table 2 reports the BP86/6-31G(d,p) strain and interaction energies for these 2.2 Å geometries. Table 2 also reports the BP86/TZP activation-strain analysis. The ΔE_{INT} dissection analysis showed consistent results for basis sets of triple-ξ quality or larger. Because a series of comparable geometries were analyzed, the impact of the interaction energy on controlling the heteroaromatic and ethylene strain energy can be assessed. The ΔE_{STRAIN} energies decrease from 29.7 kcal/mol in reaction 1 to 18.8 kcal/mol in reaction 5. This decrease results from a 7.5 kcal/mol decrease for the 1,2,4,5-tetrazine ring strain compared to benzene and a 3.4 kcal/mol decrease for ethylene distortion.[44] Radom and co-workers have previously analyzed the strain associated with heteroaromatic ring distortion in addition reactions with dihydrogen.[59] The lower strain energies for heteroaromatic azadienes compared to

dx.doi.org/10.1021/jo5025514 | J. Org. Chem. 2015, 80, 548−558

benzene were correlated to the intramolecular ring distance between atom centers involved in bond formation. The introduction of nitrogen atoms shortens the relative 1,4-intramolecular ring distance. For example, the BP86/6-31G(d,p) C1−C4 distance in the ground state of benzene is 2.809 Å, while the C3−C6 distance in the ground state of 1,2,4,5,-tetrazine is 2.542 Å. Constraining flat benzene and 1,2,4,5,-tetrazine to their 2.2 Å geometry bond lengths indicates that less than 3 kcal/mol of the heteroarene strain energy is due to bond length changes. The majority of the heteroarene strain energy is due to ring puckering that is required to achieve the transition-state geometry, which as suggested by Radom and co-workers, is highly influenced by the 1,4-intramolecular ring distance. Interestingly, in reaction 1, benzene distorts to decrease the C1−C4 distance to 2.479 Å in the 2.2 Å geometry, while in reaction 5, 1,2,4,5,-tetrazine distorts to increase the C3−C6 distance to 2.687 Å in the 2.2 Å geometry.

While a decrease in activation-strain energy is responsible for lowering part of the activation energy from benzene through 1,2,4,5-tetrazine, the increase in stabilizing interaction energy is larger than the decrease in this distortion-induced strain energy and is more important for reactions 1−5 (Table 2). The BP86/6-31G(d,p) ΔE_{INT} values change from 2.7 kcal/mol repulsive in reaction 1 to −14.3 kcal/mol stabilizing in reaction 5. For 1,2,4,5-tetrazine, the 17.0 kcal/mol more stabilizing interaction energy combined with the 10.9 kcal/mol lower strain energy decreases the ΔE by 27.9 kcal/mol compared to benzene.

What is the origin of the large strengthening in ΔE_{INT} for 1,2,4,5-tetrazine compared to benzene? As outlined in the Introduction, it is assumed that occupied−unoccupied orbital interactions that allow electron density to delocalize from ethylene onto 1,2,4,5-tetrazine in the transition state are responsible. However, the activation-strain analysis and breakdown of the interaction energy into its physical components indicates that this is incorrect. Columns 5−8 in Table 2 report the BP86/TZP interaction energy and dissection of the interaction energy into its physical components. Column 5 in Table 2 reports the orbital energy stabilization (ΔE_{ORB}) that results from frontier HOMO−LUMO and all other occupied−unoccupied interactions. Unexpectedly, the ΔE_{ORB} values are nearly constant, and therefore, orbital interactions are not the origin of fast 1,2,4,5-tetrazine reactivity. Electrostatic interactions are also not the origin of the enhanced interaction energy in reaction 5. Electrostatic attraction becomes less stabilizing from reaction 1 to reaction 5 (see column 6).

The origin of enhanced stabilization between the 1,2,4,5-tetrazine and ethylene versus benzene and ethylene is a significant decrease in Pauli repulsion. This destabilizing interaction results from closed-shell electron repulsion between occupied orbitals of the heteroarene interacting with occupied orbitals of ethylene. Column 7 of Table 2 shows that the ΔE_{PAULI} energies decrease from a penalty of 114.0 kcal/mol in reaction 1 to a penalty of 89.3 kcal/mol for reaction 5. Closed-shell repulsion was not previously considered as the origin of fast inverse-electron-demand Diels−Alder reactions because simple FMO theory neglects this repulsion. Our conclusion is in accord with early work by Bach and co-workers, who used Hartree−Fock calculations and identified that closed-shell repulsion is responsible for the large activation barrier for cycloaddition of 1,3-butadiene with ethylene.[60−62] Closed-shell repulsion also accounts for the large activation of acetylene trimerization[63,64] and has been implicated in other types of organic reactions,[65,66] such as S_N2 reactions.[67]

Why Closed-Shell Repulsion Decreases. Why does closed-shell repulsion between the heteroarene and ethylene decrease upon substitution of nitrogen atoms for CH groups? From a qualitative perspective, decreased repulsion can be expected because the more electronegative nitrogen atoms polarize the π electrons away from the carbon atoms involved in C−C bond formation during cycloaddition. To identify which occupied−occupied orbital interactions that are responsible for the trend in closed-shell repulsion, we analyzed orbital energy changes between the distorted heteroarene and the distorted ethylene fragments at the 2.2 Å geometries with deletion of all unoccupied orbitals. This deletion prevents all occupied−unoccupied orbital interactions, and orbital energy changes are due only to electrostatic interactions and closed-shell Pauli repulsion. Figure 4 shows the most important π orbitals and their energy changes that occur upon interaction between benzene and ethylene. The solid lines show the energy changes that occur from electrostatic and closed-shell repulsion, whereas the dashed lines show the energy changes that occur from occupied−unoccupied orbital interactions. These one-electron orbital changes provide qualitative insight into the total Pauli repulsion and total orbital interaction energy.

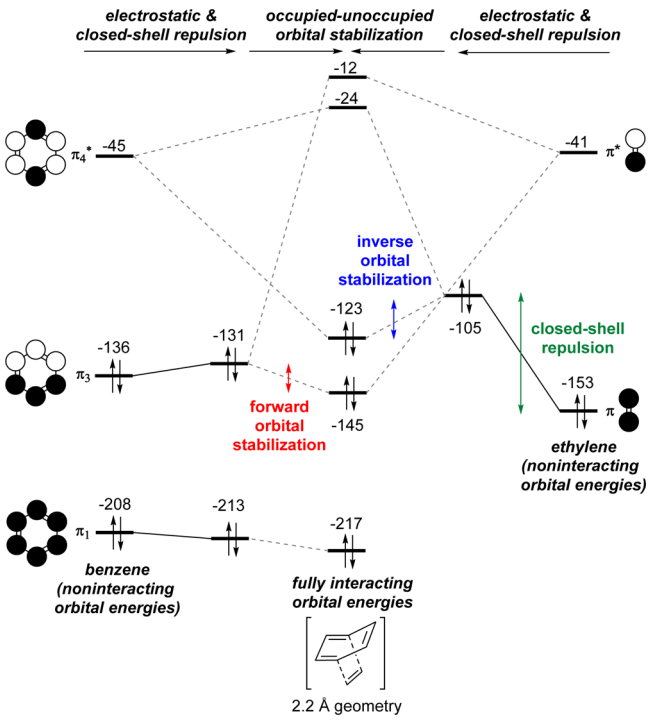

Figure 4. Orbital energy changes for interaction between benzene and ethylene. Solid lines connect orbital energy levels with deletion of all unoccupied orbitals. Dashed lines connect orbital energy levels after occupied−unoccupied interactions are included. Orbital energies reported in kcal/mol.

Figure 4 reveals that the energetically most impactful closed-shell repulsion occurs between the ethylene π orbital and the lowest energy π_1 orbital of benzene.[60] This interaction destabilizes the ethylene π electrons by 48 kcal/mol. The frontier π_3 orbital is not destabilized by closed-shell repulsion since it is orthogonal to the ethylene π orbital. Comparison to the same interaction between 1,2,4,5-tetrazine and ethylene shows only a 2 kcal/mol energy destabilization for the interaction of the ethylene π orbital and π_1 orbital of 1,2,4,5-

dx.doi.org/10.1021/jo5025514 | J. Org. Chem. 2015, 80, 548−558

tetrazine (Figure 5). The decrease in closed-shell repulsion and decrease in activation barrier is reminiscent of a similar case for

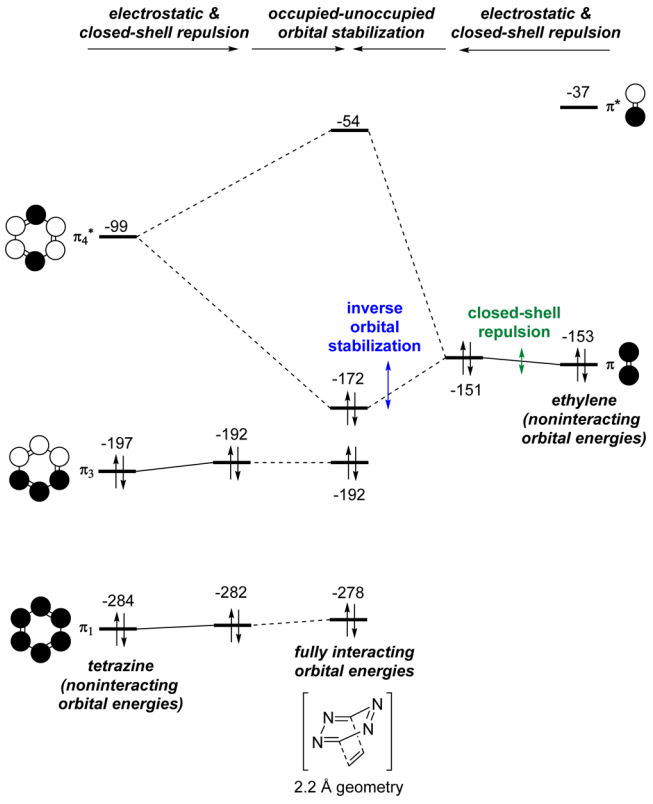

Figure 5. Orbital energy changes for interaction between 1,2,4,5-tetrazine and ethylene. Solid lines connect orbital energy levels with deletion of all unoccupied orbitals. Dashed lines connect orbital energy levels after occupied−unoccupied interactions are included. Orbital energies reported in kcal/mol.

Pd metal-mediated carbon−halogen bond activation that benefits from anion assistance.[68]

Why Frontier Orbital Interactions Do Not Control Activation Energies. One unexpected result from the activation-strain values reported in Table 2 is that the ΔE_{ORB} values are nearly identical in reactions 1−5. This orbital energy stabilization is the result of all occupied−unoccupied interactions, but it is generally expected that frontier interactions should dominate. There are multiple possibilities why the ΔE_{ORB} values are nearly constant. (1) The inverse frontier orbital energy gap decreases, but there is a corresponding increase in the forward frontier orbital energy gap that is offsetting. (2) The frontier orbital energies show the expected increase in stabilization, but nonfrontier orbital interactions diminish this effect.

Figures 4 and 5 compare the effects of the orbital energies before and after occupied−unoccupied orbital interactions. The benzene HOMO to ethylene LUMO interaction results in stabilizing the π_3 electrons by 14 kcal/mol, and the ethylene HOMO to benzene LUMO interaction results in 18 kcal/mol of stabilization. These nearly equal interactions are expected based on FMO theory. For the interaction of 1,2,4,5-tetrazine with ethylene, the 1,2,4,5-tetrazine HOMO to ethylene LUMO interaction results in essentially no stabilization, while the ethylene HOMO to 1,2,4,5-tetrazine LUMO interaction results in 21 kcal/mol of stabilization. This suggests that, while the inverse FMO interaction does become more stabilizing for 1,2,4,5-tetrazine, the decrease in the forward FMO interaction is offsetting. Nonfrontier occupied−unoccupied orbital interactions also contribute to this effect, but to a minor extent.

Origin of Kinetic−Thermodynamic Relationship. The kinetic−thermodynamic relationship for heteroarene−ethylene cycloadditions is somewhat unique since a similar relationship for cycloaddition between heteroarenes and dihydrogen does not exist.[44,59] Therefore, we wondered whether this kinetic−thermodynamic relationship is fortuitous or results from a trend in closed-shell repulsion similar to that found for the activation energies.

Table 3 reports the dissection of the interaction energy between the heteroarene and ethylene fragments in the cycloadduct geometry. The electronic configuration of the product for the energy decomposition analysis mirrors the transition-state electronic configuration (i.e., closed-shell configuration). As expected, the interaction energies for the cycloadducts are significantly more stabilizing than in the cycloaddition transition states. The trend in total interaction energies and the components of the interaction energies are very similar to the 2.2 Å and transition-state geometries. For the cycloadducts, the interaction energy increases in stabilization by 16.3 kcal/mol from reaction 1 to reaction 5, which is identical to the change found in the 2.2 Å geometries. Similarly, the ΔE_{ORB} values are nearly constant and there is a decrease in stabilization of the ΔE_{ELSTAT} values. The ΔE_{PAULI} values show a 30.7 kcal/mol decrease in repulsion comparing reactions 1 and 5, which is comparable to the 24.7 kcal/mol change found in the 2.2 Å geometries. This decrease in closed-shell repulsion offsets the decrease in electrostatic interactions and accounts for the change in ΔE_{INT}. A plot of the ΔE_{PAULI} values for the

Table 3. BP86/TZP Components of Interaction Energy for Cycloadducts in Reactions 1−5[a]

	ΔE_{ORB}	ΔE_{ELSTAT}	ΔE_{PAULI}	ΔE_{INT}
Rxn 1: benzene cycloadduct (1,4-addition)	−368.8	−231.5	473.0	−127.3
Rxn 2: pyridine cycloadduct (2,5-addition)	−368.4	−228.8	465.7	−131.5
Rxn 3: pyridazine cycloadduct (3,6-addition)	−387.8	−229.4	464.7	−143.5
Rxn 4: 1,2,4-triazine cycloadduct (3,6-addition)	−372.4	−223.8	453.8	−142.2
Rxn 5: 1,2,4,5-tetrazine cycloadduct (3,6-addition)	−369.0	−216.9	442.3	−143.6

[a]Energies are reported in kcal/mol.

dx.doi.org/10.1021/jo5025514 | J. Org. Chem. 2015, 80, 548−558

Table 4. BP86/TZP Activation-Strain Analysis for Regioisomers of Reactions 1−5[d]

	ΔE^a	$\Delta E_{STRAIN}{}^a$	$\Delta E_{INT}{}^a$	$\Delta E_{ORB}{}^b$	$\Delta E_{ELSTAT}{}^b$	$\Delta E_{PAULI}{}^b$	$\Delta E_{INT}{}^b$	S^c
pyridine:1,4-addition	36.8	24.9	11.9	−45.0	−51.3	111.3	14.9	0.16
Δ (2,5-addition)	10.4	−2.9	13.3	10.3	0.9	3.3	14.4	−0.04
pyridazine:1,4-addition	28.7	23.5	5.1	−48.1	−49.4	104.6	7.1	0.17
Δ (3,6-addition)	8.2	−2.1	10.3	6.8	0.3	3.0	10.1	−0.04
1,2,4-triazine: 2,5-addition	20.3	21.1	−0.8	−49.6	−47.5	98.4	1.3	0.18
Δ (3,6-addition)	7.4	−1.8	7.3	5.9	0.2	2.8	5.8	−0.04
1,2,4-triazine: 1,4-addition	17.0	4.7	12.3	−39.5	−46.8	100.8	14.5	0.13
Δ (3,6-addition)	4.1	−18.2	20.4	16.0	0.9	5.2	22.1	−0.09
1,2,4,5-tetrazine: 1,4-addition	18.7	15.4	3.4	−43.9	−45.4	95.1	5.8	0.14
Δ (3,6-addition)	14.1	−3.4	17.7	11.9	−0.1	5.8	17.6	−0.09

[a]BP86/6-31G(d,p). [b]BP86/TZP. [c]Orbital overlap between ethylene HOMO and azadiene LUMO. [d]Geometries are constrained at 2.2 Å for the forming bonds. Energies are reported in kcal/mol.

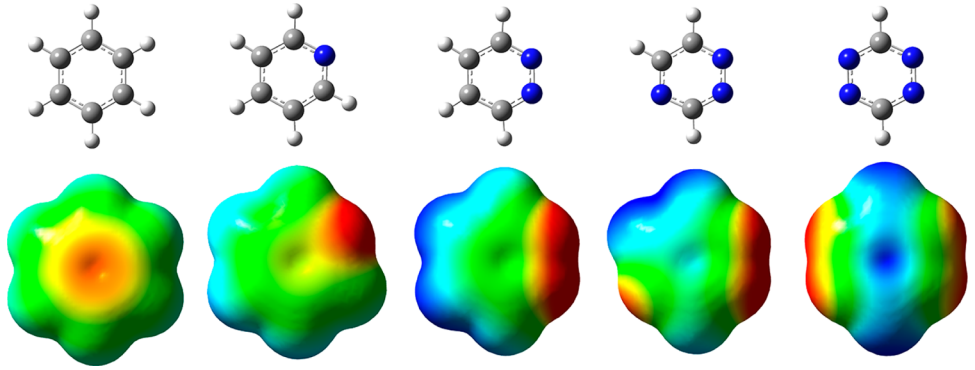

Figure 6. Comparison of ground-state molecular electrostatic potentials (ESPs) for benzene and heteroaromatic azadienes (BP86/6-31G(d,p) values plotted from −3.4e-2 (red) to +3.4e-2 (blue) Hartree).

2.2 Å geometries versus the cycloadduct geometries for reactions 1−5 shows a linear correlation with an R^2 value of 0.93. This indicates that the kinetic−thermodynamic relationship is indeed the result of similar physical interactions and that the interactions in the 2.2 Å geometries are magnified in the cycloadduct geometries.

Regioselectivity and C−C versus C−N Bond Formation. Our calculations, as well as previous calculations by Ho and Li,[40] show that there is significant regioselectivity that favors C−C bond formation over C−N bond formation. Ho and Li attributed this preference to more efficient orbital overlap and a more stabilizing resonance integral between the interaction of carbon atoms versus the interaction of a carbon and a nitrogen atom or two nitrogen atoms, although no direct evaluation of orbital overlap or resonance integrals was reported. Similarly, Radom and co-workers suggested that, for H_2 addition to heteroarenes, H−C bond formation is favored over H−N bond formation because the more electronegative nitrogen atoms have more contracted π orbitals and less orbital overlap.[59]

Table 4 reports the activation-strain analysis for regioisomer geometries with forming partial bonds constrained to 2.2 Å. The energy and overlap differences (Δ) compared to the lowest energy regioisomer are also given. Inspection of the ΔE_{STRAIN} terms reveals that the higher energy regioisomer reactions pay ∼2−3 kcal/mol less strain energy than the lower energy regioisomer structure. This means that regioselectivity can be almost completely attributed to the interaction energy ΔE_{INT} between the azadiene and ethylene.

While the relative reactivity of heteroaromatic azadienes is controlled by closed-shell repulsion, this interaction does not determine regioselectivity. The energies in Table 4 indicate that the higher energy regioisomer geometry has a nearly constant 3−5 kcal/mol higher energy closed-shell repulsion energy. Also, the electrostatic interactions ΔE_{ELSTAT} are not significantly different between regioisomeric geometries. Instead, the difference in interaction energies is almost entirely due to occupied−unoccupied orbital interactions, ΔE_{ORB}.[69] For example, the ΔE_{INT} value in the 3,6-addition geometry of 1,2,4,5-tetrazine with ethylene is −11.8 kcal/mol stabilizing. For 1,4-addition, the ΔE_{INT} value is 5.8 kcal/mol destabilizing, which is a change of 17.6 kcal/mol. The corresponding change in ΔE_{ORB} is 11.9 kcal/mol.

The differences in ΔE_{ORB} values for regioisomer geometries can be attributed to intermolecular frontier orbital overlap (S). Tables 2 and 4 report the calculated orbital overlap between the ethylene HOMO and the unoccupied heteroarene LUMO. This orbital overlap values range from S = 0.13 to 0.18 for the higher energy regioisomer geometries and range from S = 0.20 to 0.23 for the lower energy regioisomer geometries.

New Model and Reactivity Predictor. The discovery that the relative reactivity of heteroaromatic azadienes in inverse-electron-demand cycloaddition reactions with alkenes is determined by closed-shell Pauli repulsion provides a new predictive model. In a perturbation approach, repulsion energy due to the overlap of filled orbitals is approximately proportional to (1) the amplitude of the fragment molecular orbitals, and (2) the square of the overlap integral.[70] Note that repulsion energy does not depend on the energy gap between the occupied orbitals, but is, however, proportional to the sum of fragment orbital energies; that is, higher energy occupied orbitals lead to stronger repulsion.[34a,70] This indicates that one

dx.doi.org/10.1021/jo5025514 | J. Org. Chem. 2015, 80, 548−558

straightforward predictor of relative reactivity is the occupied wave function amplitude and, therefore, the electron density at the atoms involved in bond formation. For the reactions examined here, decreasing the electron density at the carbon atoms of the heteroaromatic azadiene decreases the Pauli repulsion with the alkene cycloaddition partner and lowers the activation barrier.

One convenient way to evaluate the relative electron population of the heteroaromatic azadiene atoms involved in bond formation during cycloaddition with ethylene is to calculate and display the molecular electrostatic potentials (ESPs). While qualitative, this strategy provides a useful prediction device of relative wave function amplitude and electron density. Molecular ESPs are also advantageous because they are generally not highly method and basis set dependent. Figure 6 displays the ESP plots for benzene and heteroaromatic azadiene ground-state structures. Examination of the carbon atoms involved in bond formation with ethylene shows a clear change in electron density as adjacent CH groups are replaced with nitrogen atoms. This is especially evident comparing the carbon atoms in benzene with the carbon atoms in 1,2,4,5-tetrazine. This qualitatively predicts that, for 1,2,4,5-tetrazine reaction with alkenes, there will be diminished closed-shell repulsion and increased reactivity.

CONCLUSIONS

The fast reactivity of heteroaromatic azadienes in inverse-electron-demand Diels–Alder reactions is not due to FMO interactions. Instead, the fast reactivity of 1,2,4,5-tetrazine compared to benzene, pyridine, and other heteroarenes is due to a decrease in closed-shell Pauli repulsion. This is supported by our activation-strain analysis in combination with quantitative molecular orbital bonding analyses to evaluate transition-state geometries and reaction pathways based on accurate DFT calculations. Analysis of orbital energies with deletion of all unoccupied orbitals reveals that the reactivity-controlling repulsion interaction occurs between the filled ethylene π orbital and the lowest energy π orbital of the heteroarene. FMO interactions do not control reactivity because, while the inverse FMO interaction becomes more stabilizing for 1,2,4,5-tetrazine compared to benzene, there is a decrease in the forward FMO interaction that is offsetting. The kinetic–thermodynamic relationship found for these inverse-electron-demand cycloadditions is also due to trends in closed-shell repulsion in the cycloadducts, which indicates that the interactions in the transition-state geometries are magnified in the cycloadduct. Unlike reactivity, regioselectivity is the result of differences in occupied–unoccupied orbital interactions due to greater orbital overlap in the lower energy C–C bond forming regioisomer geometries.

ASSOCIATED CONTENT

Supporting Information

XYZ coordinates and further computational details and analysis. This material is available free of charge via the Internet at http://pubs.acs.org.

AUTHOR INFORMATION

Corresponding Authors

*E-mail: dhe@chem.byu.edu (D.H.E.).
*E-mail: f.m.bickelhaupt@vu.nl (F.M.B.).

Notes

The authors declare no competing financial interest.

ACKNOWLEDGMENTS

We thank BYU, the Fulton Supercomputing Lab, and The Netherlands Organization for Scientific Research (NWO-CW) for financial support and computational resources. I.F. is grateful to the Spanish MINECO (grant CTQ2013-44303-P).

REFERENCES

(1) (a) Boger, D. L. *Tetrahedron* **1983**, *39*, 2869. (b) Boger, D. L. *Chem. Rev.* **1986**, *86*, 781.
(2) For select examples of heteroaromatic azadiene cycloadditions, see: (a) Boger, D. L.; Kochanny, M. J. *J. Org. Chem.* **1994**, *59*, 4950. (b) Sakya, S. M.; Groskopf, K. K.; Boger, D. L. *Tetrahedron Lett.* **1997**, *38*, 3805. (c) Boger, D. L.; Schaum, R. P.; Garbaccio, R. M. *J. Org. Chem.* **1998**, *63*, 6329. (d) Hamasaki, A.; Ducray, R.; Boger, D. L. *J. Org. Chem.* **2005**, *71*, 185. (e) Soenen, D. R.; Zimpleman, J. M.; Boger, D. L. *J. Org. Chem.* **2003**, *68*, 3593.
(3) (a) Sauer, J. *Angew. Chem.* **1967**, *79*, 76. (b) Sustmann, R. *Tetrahedron Lett.* **1971**, *29*, 2721.
(4) For select examples of nonaromatic azadienes, see: (a) Boger, D. L.; Corbett, W. L.; Curran, T. T.; Kasper, A. M. *J. Am. Chem. Soc.* **1991**, *113*, 1713. (b) Boger, D. L.; Curran, T. T. *J. Org. Chem.* **1990**, *55*, 5439.
(5) (a) Raw, S. A.; Taylor, R. J. K. *J. Am. Chem. Soc.* **2004**, *126*, 12260. (b) Benson, S. C.; Lee, L.; Yang, L.; Snyder, J. K. *Tetrahedron* **2000**, *56*, 1165. (c) Girardot, M.; Nomak, R.; Snyder, J. K. *J. Org. Chem.* **1998**, *63*, 10063. (d) Klindert, T.; Stroetmann, I.; Seitz, G.; Höfner, G.; Wanner, K. T.; Frenzen, G.; Eckhoff, B. *Arch. Pharm.* **1997**, *330*, 163.
(6) Boger, D. L.; Panek, J. S.; Duff, S. R. *J. Am. Chem. Soc.* **1985**, *107*, 5745.
(7) Boger, D. L.; Coleman, R. S. *J. Am. Chem. Soc.* **1987**, *109*, 2717.
(8) Boger, D. L.; Zhang, M. *J. Am. Chem. Soc.* **1991**, *113*, 4230.
(9) Boger, D. L.; Boyce, C. W.; Labroli, M. A.; Sehon, C. A.; Jin, Q. *J. Am. Chem. Soc.* **1999**, *121*, 54.
(10) Boger, D. L.; Wolkenberg, S. E. *J. Org. Chem.* **2000**, *65*, 9120.
(11) (a) Boger, D. L.; Brotherton, C. E. *J. Org. Chem.* **1984**, *49*, 4050. (b) Panek, J. S.; Zhu, B. *Tetrahedron Lett.* **1996**, *37*, 8151. (c) Moisan, L.; Odermatt, S.; Gombosuren, N.; Carella, A.; Rebek, J., Jr. *Eur. J. Org. Chem.* **2008**, 1673.
(12) Saracoglu, N. *Tetrahedron* **2007**, *63*, 4199.
(13) (a) Blackman, M. L.; Royzen, M.; Fox, J. M. *J. Am. Chem. Soc.* **2008**, *130*, 13518. (b) Han, H.; Devaraj, N. K.; Lee, J.; Hilderbrand, S. A.; Weissleder, R.; Bawendi, M. G. *J. Am. Chem. Soc.* **2010**, *132*, 7838.
(14) Kamber, D. N.; Nazarova, L. A.; Liang, Y.; Lopez, S. A.; Patterson, D. M.; Shih, H.-W.; Houk, K. N.; Prescher, J. A. *J. Am. Chem. Soc.* **2013**, *135*, 13680.
(15) (a) For a recent review, see: King, M.; Wagner, A. *Bioconjugate Chem.* **2014**, *25*, 825. (b) Kaya, E.; Vrabel, M.; Deiml, C.; Prill, S.; Fluxa, V. S.; Carell, T. *Angew. Chem., Int. Ed.* **2012**, *51*, 4466. (c) Lang, K.; Davis, L.; Torres-Kolbus, J.; Chou, C.; Deiters, A.; Chin, J. W. *Nat. Chem.* **2012**, *4*, 298. (d) Devaraj, N. K.; Upadhyay, R.; Haun, J. B.; Hilderbrand, S. A.; Weissleder, R. *Angew. Chem., Int. Ed.* **2009**, *48*, 7013. (e) Devaraj, N. K.; Hilderbrand, S.; Upadhyay, R.; Mazitschek, R.; Weissleder, R. *Angew. Chem., Int. Ed.* **2010**, *49*, 2869. (f) Haun, J. B.; Devaraj, N. K.; Hilderbrand, S. A.; Lee, H.; Weissleder, R. *Nat. Nanotechnol.* **2010**, *5*, 660. (g) Rossin, R.; Renart Verkerk, P.; van den Bosch, S. M.; Vulders, R. C. M.; Verel, I.; Lub, J.; Robillard, M. S. *Angew. Chem.* **2010**, *122*, 3447. (h) Keliher, E. J.; Reiner, T.; Turetsky, A.; Hilderbrand, S. A.; Weissleder, R. *ChemMedChem* **2011**, *6*, 424. (i) Li, Z.; Cai, H.; Hassink, M.; Blackman, M. L.; Brown, R. C. D.; Conti, P. S.; Fox, J. M. *Chem. Commun.* **2010**, *46*, 8043. (j) Seitchik, J. L.; Peeler, J. C.; Taylor, M. T.; Blackman, M. L.; Rhoads, T. W.; Cooley, R. B.; Refakis, C.; Fox, J. M.; Mehl, R. A. *J. Am. Chem. Soc.* **2012**, *134*, 2898. (k) Lang, K.; Davis, L.; Wallace, S.; Mahesh, M.; Cox, D. J.; Blackman, M. L.; Fox, J. M.; Chin, J. W. *J. Am. Chem. Soc.* **2012**,

134, 10317. (l) Pipkorn, R.; Waldeck, W.; Didinger, B.; Koch, M.; Mueller, G.; Wiessler, M.; Braun, K. *J. Pept. Sci.* **2009**, *15*, 235. (m) Yang, J.; Šečkutė, J.; Cole, C. M.; Devaraj, N. K. *Angew. Chem., Int. Ed.* **2012**, *51*, 7476. (n) Karver, M. R.; Weissleder, R.; Hilderbrand, S. A. *Angew. Chem., Int. Ed.* **2012**, *51*, 920. (o) Willems, L. I.; Li, N.; Florea, B. I.; Ruben, M.; van der Marel, G. A.; Overkleeft, H. S. *Angew. Chem., Int. Ed.* **2012**, *51*, 4431.

(16) Kolb, H. C.; Finn, M. G.; Sharpless, K. B. *Angew. Chem., Int. Ed.* **2001**, *40*, 2004.

(17) Rahanyan, N.; Linden, A.; Baldridge, K. K.; Siegel, J. S. *Org. Biomol. Chem.* **2009**, *7*, 2082.

(18) Devaraj, N. K.; Weissleder, R.; Hilderbrand, S. A. *Bioconjugate Chem.* **2008**, *19*, 2297.

(19) (a) Fukui, K. *Acc. Chem. Res.* **1971**, *4*, 57. (b) Fukui, K. *Angew. Chem., Int. Ed.* **1982**, *21*, 801.

(20) Boger, D. L. *Modern Organic Synthesis Lecture Notes*; TSRI Press: San Diego, CA, 1999.

(21) Houk, K. N. In *Pericyclic Reactions*; Marchand, A. P., Lehr, R. E., Eds.; Academic Press: New York, 1977; Vol. *2*, p 181.

(22) Several other studies use frontier orbital interactions to rationalize reactivity of Diels–Alder reactions. For example: Robiett, R.; Marchand-Brynaert, J.; Peeters, D. *J. Org. Chem.* **2002**, *67*, 6823.

(23) (a) Houk, K. N. *Acc. Chem. Res.* **1975**, *8*, 361. (b) Spino, C.; Pesant, M.; Dory, Y. *Angew. Chem., Int. Ed.* **1998**, *37*, 3262.

(24) For inverse-demand Diels–Alder reactions, ground-state FMO gaps often cannot predict relative reactivity trends. For example, see: Spino, C.; Rezaei, H.; Dory, Y. L. *J. Org. Chem.* **2004**, *69*, 757.

(25) For FMO use for nonaromatic azadienes, see: Venturini, A.; Joglar, J.; Fustero, S.; González, J. *J. Org. Chem.* **1997**, *62*, 3919.

(26) Liang, Y.; Mackey, J. L.; Lopez, S. A.; Houk, K. N. *J. Am. Chem. Soc.* **2012**, *134*, 17904.

(27) Gomez-Bengoa, E.; Helm, M. D.; Plant, A.; Harrity, J. P. A. *J. Am. Chem. Soc.* **2007**, *129*, 2691.

(28) Domingo, L. R.; Arnó, M.; Andrés, J. *J. Org. Chem.* **1999**, *64*, 5867.

(29) Anderson, E. D.; Boger, D. L. *J. Am. Chem. Soc.* **2011**, *133*, 12285.

(30) Herndon, W. C. *Chem. Rev.* **1972**, *72*, 157.

(31) (a) Klopman, G. *J. Am. Chem. Soc.* **1968**, *90*, 223. (b) Salem, L. *J. Am. Chem. Soc.* **1968**, *90*, 543. (c) Salem, L. *J. Am. Chem. Soc.* **1968**, *90*, 553.

(32) Morokuma, K. *J. Chem. Phys.* **1971**, *55*, 1236.

(33) Ziegler, T.; Rauk, A. *Theor. Chim. Acta* **1977**, *46*, 1.

(34) (a) Bickelhaupt, F. M.; Baerends, E. J. Kohn-Sham DFT: Predicting and Understanding Chemistry. In *Reviews in Computational Chemistry*; Lipkowitz, K.B., Boyd, D.B., Eds.; Wiley-VCH: New York, 2000; Vol. 15, pp 1–86. (b) Bickelhaupt, F. M.; Ziegler, T.; Schleyer, P. v. R. *Organometallics* **1995**, *14*, 2288. (c) Bickelhaupt, F. M. *J. Comput. Chem.* **1999**, *20*, 114.

(35) Hirao, H. *J. Comput. Chem.* **2008**, *29*, 1399.

(36) (a) Ess, D. H.; Houk, K. N. *J. Am. Chem. Soc.* **2007**, *129*, 10646. (b) Ess, D. H.; Houk, K. N. *J. Am. Chem. Soc.* **2008**, *130*, 10187. (c) Liu, F.; Paton, R. S.; Kim, S.; Liang, Y.; Houk, K. N. *J. Am. Chem. Soc.* **2013**, *135*, 15642.

(37) (a) van Zeist, W.-J.; Bickelhaupt, F. M. *Org. Biomol. Chem.* **2010**, *8*, 3118. (b) Fernández, I. *Phys. Chem. Chem. Phys.* **2014**, *16*, 7662. (c) Fernández, I.; Bickelhaupt, F. M. *Chem. Soc. Rev.* **2014**, *43*, 4953. See also: (d) Fernández, I. Understanding Trends in Reaction Barriers. In *Discovering the Future of Molecular Sciences*; Pignataro, B., Ed.; Wiley-VCH: Weinheim, 2014; pp 165–187.

(38) Frisch, M. J.; Trucks, G. W.; Schlegel, H. B.; Scuseria, G. E.; Robb, M. A.; Cheeseman, J. R.; Scalmani, G.; Barone, V.; Mennucci, B.; Petersson, G. A.; Nakatsuji, H.; Caricato, M.; Li, X.; Hratchian, H. P.; Izmaylov, A. F.; Bloino, J.; Zheng, G.; Sonnenberg, J. L.; Hada, M.; Ehara, M.; Toyota, K.; Fukuda, R.; Hasegawa, J.; Ishida, M.; Nakajima, T.; Honda, Y.; Kitao, O.; Nakai, H.; Vreven, T.; Montgomery, J. A., Jr.; Peralta, J. E.; Ogliaro, F.; Bearpark, M.; Heyd, J. J.; Brothers, E.; Kudin, K. N.; Staroverov, V. N.; Kobayashi, R.; Normand, J.; Raghavachari, K.; Rendell, A.; Burant, J. C.; Iyengar, S. S.; Tomasi, J.; Cossi, M.; Rega, N.; Millam, N. J.; Klene, M.; Knox, J. E.; Cross, J. B.; Bakken, V.; Adamo, C.; Jaramillo, J.; Gomperts, R.; Stratmann, R. E.; Yazyev, O.; Austin, A. J.; Cammi, R.; Pomelli, C.; Ochterski, J. W.; Martin, R. L.; Morokuma, K.; Zakrzewski, V. G.; Voth, G. A.; Salvador, P.; Dannenberg, J. J.; Dapprich, S.; Daniels, A. D.; Farkas, Ö.; Foresman, J. B.; Ortiz, J. V.; Cioslowski, J.; Fox, D. J. *Gaussian 09*, Revision B.01; Gaussian, Inc.: Wallingford, CT, 2009.

(39) (a) Baerends, E. J.; et al. *ADF2013.01*; SCM, Theoretical Chemistry, Vrije Universiteit: Amsterdam, 2013. See: www.scm.com. (b) te Velde, G.; Bickelhaupt, F. M.; Baerends, E. J.; Fonseca Guerra, C.; van Gisbergen, S. J. A.; Snijders, J. G.; Ziegler, T. *J. Comput. Chem.* **2001**, *22*, 931.

(40) Ho, H.-O.; Li, W.-K. *J. Mol. Struct.: THEOCHEM* **2005**, *723*, 195.

(41) Šakić, D.; Vrček, V. *J. Phys. Chem. A* **2012**, *116*, 1298.

(42) Yu, Z.-X.; Dang, Q.; Wu, Y.-D. *J. Org. Chem.* **2005**, *70*, 998.

(43) Fleming, I. *Frontier Orbitals and Organic Chemical Reactions*; Wiley: London, 1976.

(44) (a) Hayden, A.; Houk, K. N. *J. Am. Chem. Soc.* **2009**, *131*, 4084. (b) Houk and co-workers recently used the distortion/interaction model to analyze the origin of substituent and strain effects for cycloadditions between 1,2,4,5-tetrazines and alkene and alkyne dieneophiles. See: Liu, F.; Liang, Y.; Houk, K. N. *J. Am. Chem. Soc.* **2014**, *136*, 11483.

(45) (a) Bell, R. P. *Proc. R. Soc. London, Ser. A* **1936**, *154*, 414. (b) Evans, M. G.; Polanyi, M. *Trans. Faraday Soc.* **1938**, *34*, 11.

(46) Sadasivam, D. V.; Prasad, E.; Flowers, R. A., II; Birney, D. A. *J. Phys. Chem. A* **2006**, *110*, 1288.

(47) Wang, Y.; Wu, J. I-C.; Li, Q.; Schleyer, R. v. R. *Org. Lett.* **2010**, *12*, 4824.

(48) Wiberg, K. B.; Nakaji, D.; Breneman, C. M. *J. Am. Chem. Soc.* **1989**, *111*, 4178.

(49) (a) Bird, C. W. *Tetrahedron* **1992**, *48*, 335. (b) Bird, C. W. *Tetrahedron* **1996**, *52*, 9945. (c) Bird, C. W. *Tetrahedron* **1997**, *53*, 13111.

(50) (a) Fernández, I.; Frenking, G. *Faraday Discuss.* **2007**, *135*, 403. (b) Fernández, I.; Frenking, G. *Chem.—Eur. J.* **2007**, *13*, 5873.

(51) One aromaticity scale suggests that tetrazine has ∼7 kcal/mol lower aromatic stabilization energy (ASE) compared to benzene, but this is significantly less than the differences in activation energies. See: Bao, P.; Yu, Z.-H. *J. Phys. Chem. A* **2007**, *111*, 5304.

(52) Schleyer, P. v. R.; Wu, J. I.; Cossío, F. P.; Fernández, I. *Chem. Soc. Rev.* **2014**, *43*, 4909.

(53) Bachrach, S. M.; White, P. B. *J. Mol. Struct.: THEOCHEM* **2007**, *819*, 72.

(54) (a) Fernández, I.; Sierra, M. A.; Cossío, F. P. *J. Org. Chem.* **2007**, *72*, 1488. (b) Fernández, I.; Cossío, F. P.; de Cózar, A.; Lledós, A.; Mascareñas, J. L. *Chem.—Eur. J.* **2010**, *16*, 12147. (c) Andrada, D. M.; Granados, A. M.; Solà, M.; Fernández, I. *Organometallics* **2011**, *30*, 466. (d) Fernández, I.; Solà, M.; Bickelhaupt, F. M. *Chem.—Eur. J.* **2013**, *19*, 7416.

(55) (a) Fernández, I.; Bickelhaupt, F. M.; Cossío, F. P. *Chem.—Eur. J.* **2009**, *15*, 13022. (b) Fernández, I.; Cossío, F. P.; Bickelhaupt, F. M. *J. Org. Chem.* **2011**, *76*, 2310. (c) Faza, O. N.; López, C. S.; Fernández, I. *J. Org. Chem.* **2013**, *78*, 5669.

(56) Chen, Z.; Wannere, C. S.; Corminboeuf, C.; Puchta, R.; Schleyer, P. v. R. *Chem. Rev.* **2005**, *105*, 3842.

(57) Bader, R. F. W. *Atoms in Molecules: A Quantum Theory*; Clarendon: Oxford, U.K., 1990.

(58) (a) Fallah-Bagher-Shaidaei, H.; Wannere, C. S.; Corminboeuf, C.; Puchta, R.; Schleyer, P. v. R. *Org. Lett.* **2006**, *8*, 863. (b) Herges, R.; Geuenich, D. *J. Phys. Chem. A* **2001**, *105*, 3214. (c) Geuenich, D.; Hess, K.; Köhler, F.; Herges, R. *Chem. Rev.* **2005**, *105*, 3758.

(59) Zhong, G.; Chan, B.; Radom, L. *J. Am. Chem. Soc.* **2007**, *129*, 924.

(60) Bach, R. D.; McDouall, J. J. W.; Schlegel, H. B.; Wolber, G. J. *J. Org. Chem.* **1989**, *54*, 2931.

(61) Townshend, R. E.; Ramunni, G.; Segal, G.; Hehre, W. J.; Salem, L. *J. Am. Chem. Soc.* **1976**, *98*, 2190.

(62) Caramella, P.; Houk, K. N.; Domelsmith, L. N. *J. Am. Chem. Soc.* **1977**, *99*, 4511.
(63) Bach, R. D.; Wolber, G. J.; Schlegel, H. B. *J. Am. Chem. Soc.* **1985**, *107*, 2837.
(64) Houk, K. N.; Gandour, R. W.; Strozier, R. W.; Rondan, N. G.; Paquette, L. A. *J. Am. Chem. Soc.* **1979**, *101*, 6797.
(65) Bach, R. D.; Wolber, G. J. *J. Am. Chem. Soc.* **1984**, *106*, 1401.
(66) Vektariene, A. *J. Phys. Chem. A* **2013**, *117*, 8449.
(67) (a) van Bochove, M. A.; Swart, M.; Bickelhaupt, F. M. *J. Am. Chem. Soc.* **2006**, *128*, 10738. (b) Bento, A. P.; Bickelhaupt, F. M. *J. Org. Chem.* **2007**, *72*, 2201.
(68) Diefenbach, A.; de Jong, G. T.; Bickelhaupt, F. M. *J. Chem. Theory Comput.* **2005**, *1*, 286.
(69) Houk, K. N. *J. Am. Chem. Soc.* **1973**, *95*, 4092.
(70) Albright, T.; Burdett, J. K.; Whangbo, M.-H. *Orbital Interactions in Chemistry*, 2nd ed.; John Wiley & Sons: Hoboken, NJ, 2013.

■ NOTE ADDED AFTER ASAP PUBLICATION

Reference 44b was added December 9, 2014.